Supplemental Material for

Exercise hormone irisin mitigates endothelial barrier dysfunction and microvascular leakage related diseases

Jianbin Bi, Jia Zhang, Yifan Ren, Zhaoqing Du, Yuanyuan Zhang, Chang Liu, Yawen Wang, Lin Zhang, Zhihong Shi, Zheng Wu, Yi Lv, Rongqian Wu

Supplementary Figures

Figure S1. Irisin restored endothelial barrier function in LPS-induced microvascular leakage. Irisin was given by intravenous administration (250 μg/kg, a single dose) immediately after LPS administration. The vehicle group of mice was given equivalent amounts of saline. 24 h after LPS administration, lung samples were collected and transmission electron microscopy (TEM) was performed. Arrows represents the connections between endothelial cells (scale bar = 1 μm).

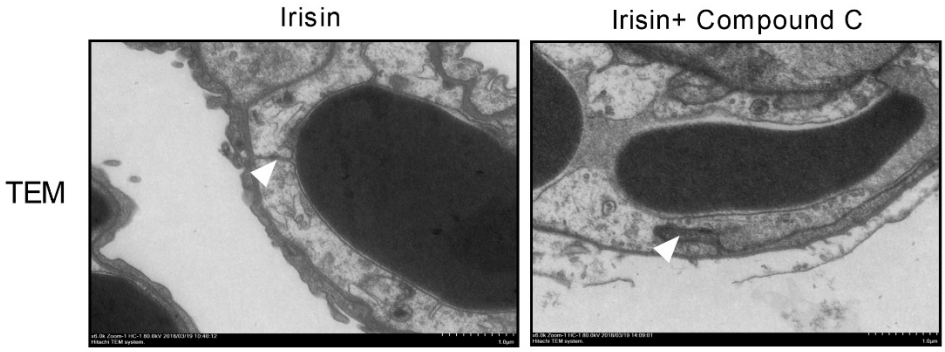

Figure S2. Exogenous irisin decreased bronchoalveolar lavage fluid (BALF) and serum inflammatory cytokine levels in CLP-induced sepsis. Irisin was given by intravenous administration (250 μg/kg, a single dose) immediately after CLP operation. The vehicle group of mice was given equivalent amounts of saline. 21 h after CLP operation, BALF and blood samples were collected. (A-C) Tumor necrosis factor α (TNF-α), macrophage inflammatory protein (MIP-2) and cold-inducible RNA binding protein (CIRP) levels in the BALF, respectively; (D-F) Serum TNF-α, MIP-2 and CIRP levels, respectively; n=6 per group, mean ± SEM, *P < 0.05 versus the sham group, #P < 0.05 versus the CLP group; One-way ANOVA was used to analyze the differences between groups.

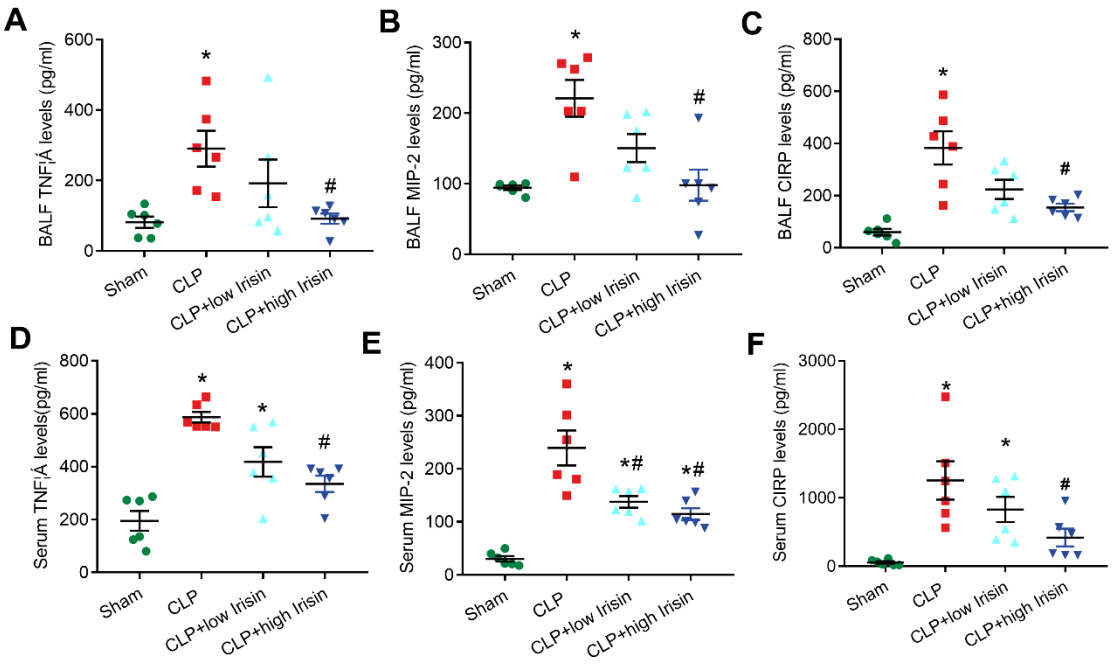

Figure S3. Exogenous irisin alleviated gut/liver ischemia reperfusion-induced lung microvascular leakage. Irisin was given by intravenous administration (250 μg/kg, a single dose) at the beginning of gut/liver reperfusion. The vehicle group of mice was given equivalent amounts of saline. 4 h after gut ischemia reperfusion (gut IR) and 24 h after liver ischemia reperfusion, lungs were collected. (A) Body weight changes; (B) Water content in lungs in gut IR-induced ALI; (C) Water content in lungs in liver IR-induced ALI; (D) Hematoxylin and eosin staining (H&E) in gut IR-induced ALI (scale bar = 20 μm); (E) ALI score in gut IR-induced ALI; (F) H&E staining in liver IR-induced ALI (scale bar = 20 μm); (G) ALI scores in liver IR-induced ALI; n=6 per group, mean ± SEM, *P < 0.05 versus the sham group, #P < 0.05 versus the gut IR or liver IR group; One-way ANOVA was used to analyze the differences between groups.

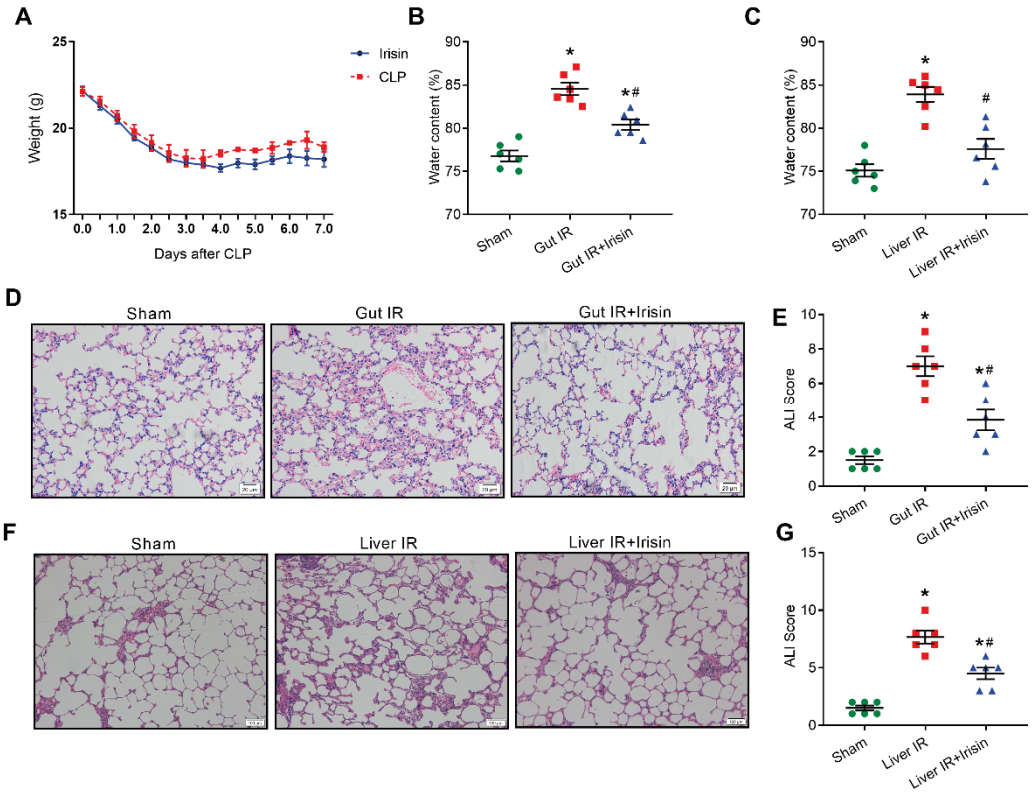

Figure S4. Exogenous irisin administration relieved pulmonary secretion of inflammatory cytokines and inflammatory cells after LPS administration. Irisin was given by intravenous administration (250 μg/kg, a single dose) immediately after LPS administration (2 mg/kg). The vehicle group of mice was given equivalent amounts of saline. 24 h after LPS treatment, lung tissues, BALF and blood samples were collected. (A-D) The number of white blood cells (WBCs), lymphocytes, monocytes and neutrophils in BALF, respectively; (E) Myeloperoxidase (MPO) immunofluorescence staining (red) and the corresponding nuclear counterstaining (blue) (scale bar = 100 μm). (F) Percentages of MPO-positive cells; (G-I) Tumor necrosis factor α (TNF-α), macrophage inflammatory protein (MIP-2) and cold-inducible RNA binding protein (CIRP) levels in BALF, respectively; (J-M) Serum TNF-α, MIP-2, CIRP and interleukin (IL)-10 levels, respectively; n=6 per group, mean ± SEM, *P < 0.05 versus the sham group, #P < 0.05 versus the LPS group; One-way ANOVA was used to analyze the differences between groups.

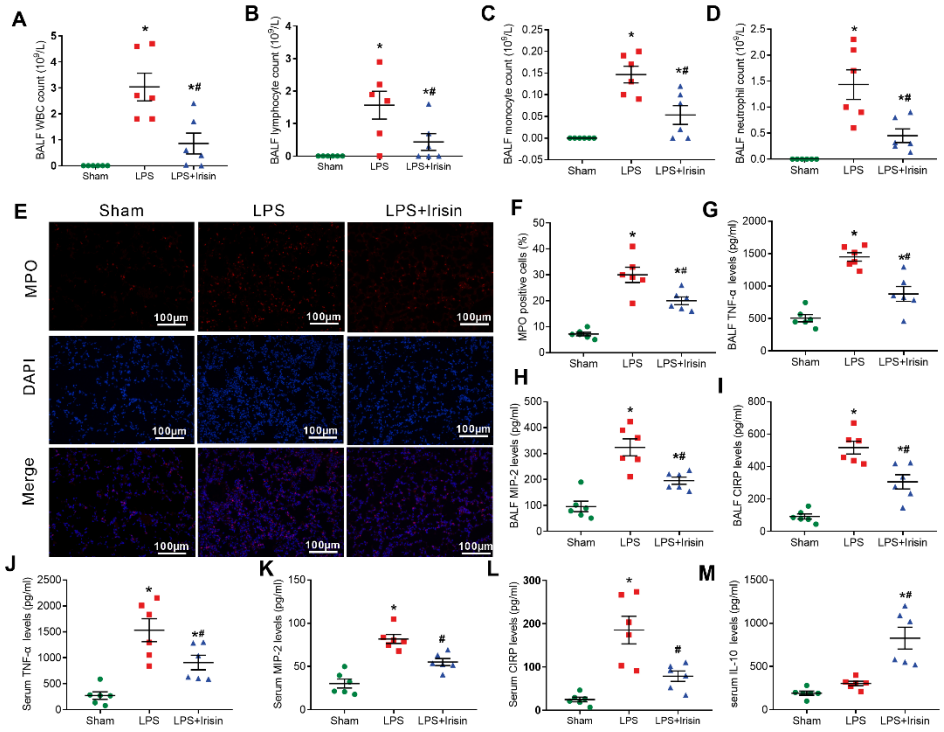

Figure S5. Irisin treatment ameliorated excessive mitochondrial fission after LPS administration. HMVECs were treated with 100 ng/ml irisin immediately after 500 ng/ml LPS administration. (A-C) Western blot analysis of the expression of dynamin related protein 1 (drp-1) and fission 1 (Fis-1) in HMVECs. n=3 per group, mean ± SEM, *P < 0.05 versus the sham group, #P < 0.05 versus the LPS group; One-way ANOVA was used to analyze the differences between groups.

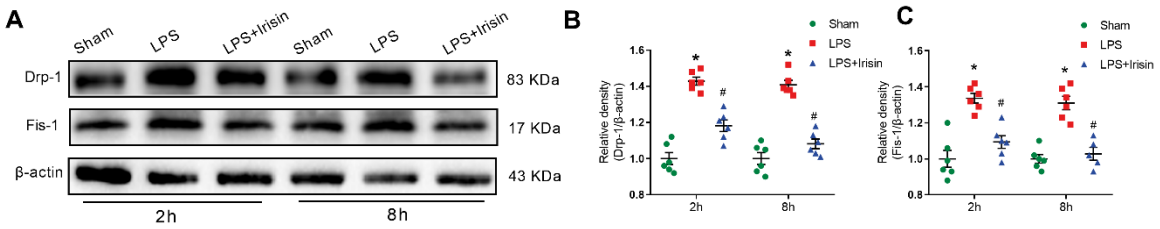

Table S1. Patient demographics

Variables	ALI patients (n=60)	Healthy individuals (n=60)
Age (years)	60.16 ± 18.60	58 ± 12.44
Sex (male/female)	33/27	35/25
BMI	21.42 ± 0.87	21.88 ± 1.09
Coexisting conditions		
Smoking, n (%)	19 (31.66)	-
Drinking, n (%)	15 (25.00)	-
Hypertension, n (%)	14 (23.33)	-
Diabetes mellitus, n (%)	9 (15.00)	-
Cirrhosis, n (%)	4 (6.67)	-
Ischemic heart disease, n (%)	6 (10.00)	-
Stroke, n (%)	3 (3.33)	-

Table S2. Risk factors of 28-day mortality by univariate and multivariate analysis

Parameters	Univariate analysis		multivariate analysis	
	HR (95% CI)	*P* value	HR (95% CI)	*P* value
Age (years)	1.041(0.992-1.093	0.106	-	-
Sex (male/ femal)	0.750(0.194-2.895)	0.676	-	-
Hypertension (yes/ no)	0.147(0.034-0.631)	**0.010**	0.323(0.030-3.524)	0.354
Diabetes (yes/ no)	3.281(0.610-17.650)	0.166	-	-
Ischemic heart disease (yes/ no)	0.818(0.141-4.765)	0.823	-	-
APACHE II score at admission	1.570(1.170-2.108)	**0.003**	1.375(1.009-1.874)	**0.044**
SOFA score at admission	2.199(1.185-4.082)	**0.012**	1.443(0.633-3.291)	0.384
Serum irisin (ng/ml)	0.210(0.071-0.622)	**0.005**	0.153(0.024-0.961)	**0.045**

Detailed methods

Murine model of LPS-induced lung microvascular leakage

A murine model of LPS-induced lung microvascular leakage was used as previously reported (1). Mice were anesthetized with isoflurane. 2 mg/kg LPS (055:B5, Sigma-Aldrich, USA) was delivered intratracheally. A sham group of mice was given equivalent amounts of PBS. Irisin (067-29A, Phoenix Pharmaceuticals, USA) was administrated by intravenous injection in mice (250 μg/kg, single dose) 0 h or 6 h after LPS model. Vehicle group of mice was given equivalent amounts of saline. Mice were euthanized 24 h after LPS treatment.

Murine model of cecal ligation and puncture (CLP)-induced sepsis

A murine model of CLP-induced sepsis was conducted as previously described (2). The mice were anesthetized with isoflurane. The cecum was exposed, ligated just distal to the ileocecal valve and punctured with a 22-gauge needle. Irisin was administrated by intravenous injection in mice (250 μg/kg, single dose) immediately after CLP operation. Vehicle group of mice was given equivalent amounts of saline. Mice were euthanized 21 h after CLP.

Murine model of gut ischemia reperfusion (gut IR)-induced lung microvascular leakage

A murine model of gut IR-induced lung microvascular leakage was generated as previously described (3). Mice were anesthetized with isoflurane. The superior mesenteric artery (SMA) was clamped with a vascular clamp for 60 min and then opened for reperfusion. Irisin was administrated by intravenous injection in mice (250 μg/kg, single dose) immediately after reperfusion. Vehicle group of mice was given equivalent amounts of saline. The mice were euthanized 4 h after gut IR.

Rat model of liver ischemia reperfusion (liver IR)-induced lung microvascular leakage

An aged rat liver IR-induced lung microvascular leakage was generated as previously described (4). The rats were anesthetized with isoflurane. 70% liver arterial/portal venous blood was interrupted by an atraumatic clip cross the portal triad, above the right lateral lobe for 40 min and then allowed to undergo reperfusion. Irisin was administrated by intravenous injection in rats (250 μg/kg, single dose) immediately after reperfusion. Vehicle group of rats was given equivalent amounts of saline. The rats were euthanized 24 h after liver IR.

Administration of compound C and cilengitide trifluoroacetate

Mice were intravenously administered 20 mg/kg compound C (S7840, Selleck, China) immediately after LPS administration intratracheally. Mice were intravenously administered 20 mg/kg cilengitide trifluoroacetate (S707, Selleck, China) in mice.

Cell culture

Human microvascular endothelial cells (HMVECs), isolated from pulmonary circulations, were purchased from BeNa Culture Collection (BNCC337720, China). Human umbilical vein endothelial cells (HUVECs) were purchased from ScienCell Research Laboratories (8000, USA). Endothelial cells were cultured in endothelial cell medium (1001, ScienCell Research Laboratories, USA). Cells were incubated at 37°C with 100% humidity in 5% CO_2.

Depletion of AMPK

AMPK-specific small interfering RNA (siRNA) was obtained from GenePharma (Shanghai, China) with the following sequences: 5'- CGGGAUCAGUUAGCAACUATT-3' and 5'- UAGUUGCUAACUGAUCCCGTT -3'. Transfection of HMVECs with siRNA was performed as previously described (5). Nonspecific siRNA was used as a control treatment. After 48 h of transfection, cells were used for subsequent experiments.

Measurement of transendothelial electrical resistance (TER)

TER of cells was measured using an electrical cell-substrate impedance sensing system (Applied Biophysics, USA) as previously described (5)

Transwell permeability assays

Permeability of fluorescein isothiocyanate (FITC)-labeled albumin across HMVEC and HUVEC monolayers grown on 6.5 mm Transwell dishes with 0.4 μm pore polycarbonate membrane inserts (3413, Corning, USA) was assessed with a Varioskan™ LUX multifunction micro orifice plate reader (Thermo Scientific™).

Arterial blood gas analysis

Mice were anesthetized with isoflurane. Arterial blood was obtained from the abdominal aorta, and PaO2 and PaCO2 were determined via blood gas analyzer (ABL90 FLEX, Radiometer, USA).

Water content

Lung tissues were dried in a 60°C oven for 48 h. Lung water levels were calculated as H2O % =

(1 – dry weight/wet weight) × 100%.

Determination of bronchoalveolar lavage fluid (BALF) proteins

After mouse euthanasia, the lungs were lavaged three times with 1 ml cold PBS through a polyethylene tube inserted into the trachea. Recovered BALF was centrifuged at 200xg for 5 min, and the supernatant was collected. BALF total protein concentrations were measured by BCA protein assay kits (P0009, Beyotime Biotechnology, China) with a Varioskan™ LUX multifunction micro orifice plate reader (Thermo Scientific™).

Determination of BALF cells.

The recovered BALF samples were obtained, and total cell numbers were counted with an automated cell counter (TC20, Bio-Rad, Hercules, CA, USA). The white blood cell (WBC), neutrophil, lymphocyte and monocyte levels were measured with a blood analyzer (HEMAVET 950, Drew, USA).

Histological analysis

Hematoxylin and eosin (HE) staining was performed as previously described (2). ALI scores were calculated as the sum of the individual score grades from 0 (minimum), 1 (mild), 2 (moderate), 3 (severe) and 4 (maximum) for the following 3 items: alveolar hemorrhage, infiltration of inflammatory cells and alveolar wall thickness, ranging from 0 to 12 (6). Transmission electron microscopy was conducted as previously described (7). A representative field was chosen for analysis.

Enzyme-linked immunosorbent assays (ELISA)

The TNF-α mouse ELISA Kit (BMS607-3, Thermo Fisher Scientific, USA), cold-inducible RNA binding protein (CIRP) ELISA kit (CSB-EL005440MO, Cusabio, Wuhan, China), MIP-2/CXCL2 mouse ELISA Kit (EMCXCL2, Thermo Fisher Scientific, USA), interleukin 10 (IL10) mouse ELISA Kit (SEA056Mu, Cloud-Clone Corp USCN Life Science, China), human irisin commercial ELISA kit (SEN576Hu, Cloud-Clone Corp USCN Life Science, China) and mouse irisin commercial ELISA kit (SEN576Mu, Cloud-Clone Corp USCN Life Science, China) were used to measure the levels of serum and BALF TNF-α, CIRP, MIP-2, IL10 and irisin, according to the manufacturer's instructions.

ATP measurement

An ATP Assay Kit (S0026, Beyotime Biotechnology, China) was used to determine ATP levels according to the manufacturer's obstructions.

Western blot analysis

Western blot analysis was performed as previously described (3). A primary rabbit anti-Src antibody (GTX27950, genetex, USA, 1:1,000 dilution); rabbit anti-Src (phospho Tyr416) antibody (GTX24816, genetex, USA, 1:1,000 dilution); rabbit anti-MLCK (phospho-Tyr464) antibody (MBS9386064, Mybiosource, USA, 1:1,000 dilution); rabbit anti-beta catenin (phospho Y142) antibody (ab27798, Abcam, USA, 1:1,000 dilution); rabbit anti-AMPKα antibody (Cell Signaling Technology, USA, 1:1,000 dilution); rabbit anti-PAMPKα antibody (Cell Signaling Technology, USA, 1:1,000 dilution); rabbit anti-PGC1α antibody (GeneTex, USA, 1:200 dilution); rabbit anti-Tfam antibody (ab131607, Abcam, USA, 1:200 dilution); rabbit anti-PINK-1 antibody (Abcam, USA, 1:250 dilution); mouse anti ATP synthase β antibody (NBP2-02249, Novusbio, USA, 1:1,000 dilution); rabbit anti-UCP2 antibody (ab203244, Abcam, USA, 1:1,000 dilution); rabbit anti-Drp1 antibody (ab184247, Abcam, USA, 1:1,000 dilution); rabbit anti-Fis1 antibody (GTX111010, GeneTex, USA, 1:250 dilution) and an HRP-conjugated β-Actin mouse monoclonal antibody (HRP-60008, Proteintech， China, 1:1,000 dilution) were incubated overnight at 4°C. Then, HRP-conjugated Affinipure goat Anti-Rabbit IgG(H+L) (SA00001-2, Proteintech， China, 1:2000 dilution) or HRP-conjugated Affinipure Goat Anti-Mouse IgG(H+L) (SA00001-1, Proteintech， China, 1:2,000 dilution) were incubated for 1 h at room temperature. The protein expression was detected by a chemiluminescence system (Bio-Rad, Hercules, CA, USA). Protein quantification was performed using ImageJ2x software. The results were expressed as the relative intensity of protein/β-actin.

Coimmunoprecipitation (CO-IP)

Protein A/G PLUS-Agarose (sc-2003, santa, USA) was used for binding mouse anti‑integrin αvβ5 antibody (sc-81632, Santa, USA) and coprecipitation. Rabbit anti-irisin antibody (ab174833, Abcam, USA,1:1,000 dilution), rabbit anti-integrin αV antibody (ab179475, Abcam, USA, 1:1,000 dilution) and rabbit anti-integrin β5 antibody (ab15459, Abcam, USA, 1:1,000 dilution) were used for WB detection.

Rac1 and cdc42 activation assay

Rac1 and cdc42 activation in HMVECs was assessed with a RhoA/Rac1/Cdc42 Activation Assay Combo Kit (STA-405, Cell Biolabs, Inc., USA) according to the instructions of the manufacturer. Primary mouse monoclonal anti-Rac and anti-cdc42 antibodies were freshly diluted 1:200 in TBST.

Immunofluorescence staining

Immunofluorescence staining was performed as previously described (8). The cells or lungs were fixed with 4% paraformaldehyde. A primary rabbit anti-irisin antibody (1:200 dilution, NBP2-59680, Novus, USA), mouse anti-integrin αVβ5 antibody (sc-81632, Santa, USA, 1:50 dilution), rabbit anti-MPO antibody (Santa Cruz Biotechnology, Inc., CA, 1:200 dilution), monoclonal mouse VE-cadherin antibody (MAB9381, R&D system, USA, 1:200 dilution) and rabbit anti-beta catenin antibody (ab32572, Abcam, USA, 1:200 dilution) were incubated with samples overnight at 4°C. Alexa Fluor 488–conjugated Affinipure Goat Anti-Mouse IgG(H+L) (SA00006-1, Proteintech, China, 1:200 dilution) and Alexa Fluor 594–conjugated Donkey Anti-Rabbit IgG(H+L) (SA00006-8, Proteintech, China, 1:200 dilution) were incubated for 1 h at room temperature. Alexa Fluor™ 594 Phalloidin (A12381, Thermo Fisher Scientific, USA) was used for staining of F-actin according to the instructions of the manufacturer. The staining was observed with a confocal microscope (TCS SP8 STED 3X, Leica, Germany).

TUNEL, DHE and MitoTracker Red fluorescence staining

Lung paraffin sections were produced, and a transferase-mediated deoxyuridine triphosphate-biotin nick end labeling (TUNEL) kit (11684795910, Roche, Switzerland) was used according to the manufacturer's instructions. For mitochondria detection, HMVECs were incubated with MitoTracker Red CMXRos dye (M7512, Thermo Fisher Scientific, USA) for 20 min at a concentration of 200 nM. For ROS detection, HMVECs were incubated with Dihydroethidium (DHE) dye (D7008, Sigma-Aldrich, USA) for 30 min at a concentration of 3 μM. The stained cells were imaged with a confocal microscope (TCS SP8 STED 3X, Leica, Germany) and quantified with ImageJ2x software.

Reference

1. Bhandary YP, et al. Post-transcriptional regulation of urokinase-type plasminogen activator receptor expression in lipopolysaccharide-induced acute lung injury. *American journal of respiratory and critical care medicine*. 2009;179(4):288-98.

2. Wu R, et al. Ghrelin attenuates sepsis-induced acute lung injury and mortality in rats. *American journal of respiratory and critical care medicine*. 2007;176(8):805-13.

3. Cui T, et al. Milk fat globule epidermal growth factor 8 attenuates acute lung injury in mice after intestinal ischemia and reperfusion. *American journal of respiratory and critical care medicine*. 2010;181(3):238-46.

4. Yang J, et al. Human adrenomedullin and its binding protein attenuate organ injury and reduce mortality after hepatic ischemia-reperfusion. *Ann Surg*. 2009;249(2):310-7.

5. Huang RT, et al. Experimental Lung Injury Reduces Kruppel-like Factor 2 to Increase Endothelial Permeability via Regulation of RAPGEF3-Rac1 Signaling. *American journal of respiratory and critical care medicine*. 2017;195(5):639-51.

6. Bi J, et al. Astaxanthin alleviated acute lung injury by inhibiting oxidative/nitrative stress and the inflammatory response in mice. *Biomedicine & pharmacotherapy = Biomedecine & pharmacotherapie*. 2017;95:974-82.

7. Zhang J, et al. Serotonin deficiency exacerbates acetaminophen-induced liver toxicity in mice. *Scientific reports*. 2015;5:8098.

8. Birukova AA, et al. Iloprost improves endothelial barrier function in lipopolysaccharide-induced lung injury. *The European respiratory journal*. 2013;41(1):165-76.